

The radial velocity of the companion star in the low–mass X–ray binary 2S 0921–630: limits on the mass of the compact object[†]

P.G. Jonker^{1*}, D. Steeghs¹, G. Nelemans², M. van der Klis³

¹*Harvard–Smithsonian Center for Astrophysics, 60 Garden Street, Cambridge, MA 02138, Massachusetts, U.S.A.*

²*Institute of Astronomy, Madingley Road, CB3 0HA, Cambridge, UK*

³*Astronomical Institute “Anton Pannekoek”, University of Amsterdam, Kruislaan 403, 1098 SJ Amsterdam, The Netherlands*

20 March 2022

ABSTRACT

In this Paper we report on optical spectroscopic observations of the low-mass X-ray binary 2S 0921–630 obtained with the Very Large Telescope. We found sinusoidal radial velocity variations of the companion star with a semi-amplitude of 99.1 ± 3.1 km s^{−1} modulated on a period of 9.006 ± 0.007 days, consistent with the orbital period found before for this source, and a systemic velocity of 44.4 ± 2.4 km s^{−1}. Due to X–ray irradiation the centre–of–light measured by the absorption lines from the companion star is likely shifted with respect to the centre–of–mass. We try to correct for this using the so–called K–correction. Conservatively applying the maximum correction possible and using the previously measured rotational velocity of the companion star, we find a lower limit to the mass of the compact object in 2S 0921–630 of $M_X \sin^3 i > 1.90 \pm 0.25 M_\odot$ (1 σ errors). The inclination in this system is well constrained since partial eclipses have been observed in X-rays and optical bands. For inclinations between $60^\circ < i < 90^\circ$ we find $1.90 \pm 0.25 < M_X < 2.9 \pm 0.4 M_\odot$. However, using this maximum K–correction we find that the ratio between the mass of the companion star and that of the compact object, q , is 1.32 ± 0.37 implying super–Eddington mass transfer rates; however, evidence for that has not been found in 2S 0921–630. We conclude that the compact object in 2S 0921–630 is either a (massive) neutron star or a low–mass black hole.

Key words: stars: individual (2S 0921–630) — accretion: accretion discs — stars: binaries — stars: neutron — X-rays: binaries

1 INTRODUCTION

The equation of state (EoS) of neutron star matter is intimately related to the physics of the strong interactions between fundamental particles and therefore it is of great relevance in high–energy and particle physics. Theories on the EoS of neutron–star matter at supra–nuclear densities provide a firm upper limit on the mass for each EoS. The stiffer the EoS, the higher the mass limit. Neutron stars with masses well above $1.4 M_\odot$ cannot exist for so–called soft equations of state, in which matter at high densities is relatively compressible (e.g., due to meson condensation or a transition between the hadron and quark–gluon phases; cf. Lattimer & Prakash 2001). Therefore, measuring a high

mass for even one neutron star would imply the firm rejection of many proposed soft EoSs (e.g. see discussion by van Paradijs & McClintock 1995). Neutron star masses of more than $\sim 3 M_\odot$ are excluded assuming (among other things) that general relativity is the correct theory of gravity and that the velocity of sound is less than the velocity of light (Nauenberg & Chapline 1973). Therefore, a lower limit on the mass of the compact object of $3 M_\odot$ or more implies a black hole compact object.

The most accurately measured neutron star masses we have are from precise radio timing measurements of double neutron–star binaries. These empirical masses cluster around $1.35 M_\odot$ (Thorsett & Chakrabarty 1999). This is close to the mass of $1.32 M_\odot$ predicted from theoretical model calculations of Type Ib supernovae (Timmes et al. 1996). However, these double neutron star binaries are formed in high–mass X–ray binaries and due to the short life of the massive companion only a limited amount of

* email : pjonker@cfa.harvard.edu; Chandra Fellow

[†] Based on observations made with ESO Telescopes at the Paranal Observatories under programme ID 72.D–0028

matter can be accreted. In contrast, in low-mass X-ray binaries (LMXBs), the rapid rotation and low magnetic field of the neutron stars are considered evidence for much larger amounts of accreted matter (see Bhattacharya 1995 for a review). Indeed, from binary evolution models, LMXBs could accrete up to $0.7 M_{\odot}$ (e.g. van den Heuvel & Bitzaraki 1995). If so, the masses of their neutron stars could be $> 2 M_{\odot}$. Most of the constraints from timing observations of the successors of these LMXB primaries, the millisecond radio pulsars, are weak (Thorsett & Chakrabarty 1999), as the almost purely circular orbits of these systems often prevents one from measuring most of the post-Newtonian parameters that underlie the precise masses for the double-neutron star binaries. With masses of $1.57^{+0.25}_{-0.2} M_{\odot}$ and $2.2 \pm 0.4 M_{\odot}$, the msec pulsars PSR B1855+09 and PSR J0751+1807 are exceptions to this (Nice et al. 2003; Nice et al. 2004, 95% conf.).

Dynamical mass estimates or dynamically determined limits on the mass of the neutron star in LMXBs are available for the two transient sources Cen X-4 and XTE J2123-058, the Z-source Cyg X-2, and the pulsar 2S 1822-371 (Cen X-4; $M_{NS} = 1.3 \pm 0.6 M_{\odot}$ Shahbaz et al. 1993; XTE J2123-058; $M_{NS} = 1.55 \pm 0.31 M_{\odot}$ Casares et al. 2002; Cyg X-2; $M_{NS} = 1.78 \pm 0.23 M_{\odot}$ Casares et al. 1998; Orosz & Kuulkers 1999; 2S 1822-371; $M_{NS} > 1.14 \pm 0.06 M_{\odot}$; Jonker et al. 2003; Casares et al. 2003). The problem is that many of the companion stars are small, late type stars which at a distance of more than a few kpc are too faint to observe, especially since the integration times are limited to typically 1/20th of the orbital period in order to avoid Doppler smearing of the spectral lines due to the binary motion. Furthermore, the binary inclination is often poorly constrained and effects of irradiation shift the centre-of-light with respect to the centre-of-mass.

Some of the aforementioned problems will be less severe when observing long orbital period systems for which the inclination is well constrained from the fact that eclipses are observed: 2S 0921-630/V395 Car is such a high inclination LMXB with a long orbital period ($P_{orb} \approx 9.0$ days; e.g. Cowley et al. 1982, Branduardi-Raymont et al. 1983, and Mason et al. 1987). The inclination of 2S 0921-630 is relatively well constrained and must be high since partial eclipses of the compact object and accretion disc have been observed in both X-rays and optical wave bands (e.g. Branduardi-Raymont et al. 1981; Chevalier & Ilovaisky 1981; Mason et al. 1987). 2S 0921-630 is thought to be a halo object in orbit with a K0-1 III companion star; absorption lines of the companion have been detected (Branduardi-Raymont et al. 1983; Shahbaz et al. 1999). The corresponding radial velocity curve would provide a limit to the mass of the companion star. In this Paper we report on spectroscopic observations of 2S 0921-630/V395 Car.

2 OBSERVATIONS AND ANALYSIS

We observed 2S 0921-630/V395 Car with the FORS2 spectrograph mounted on the Yepun Very Large Telescope (VLT). In the period Dec 26, 2003 – Mar 13, 2004, 22 spectra using the 1200R+93 and 22 spectra using the 1028z+29 grating have been obtained in Service Mode. The exposure

time was 1300 s for each observation and a slit-width of $0.4''$ was used on each occasion. The dispersion was 0.75 \AA per pixel for the spectra obtained with the 1200R+93 grating and 0.86 \AA per pixel for the spectra obtained with the 1028z+29 grating. With a slit-width of $0.4''$ the two-pixel resolution is approximately 65 km s^{-1} at 6500 \AA . After each observing night Helium-Neon-Argon lamp wavelength calibration spectra were obtained. The seeing varied between $0.5''$ and $1.4''$ and the spectra were obtained when the source had an airmass of $\sim 1.2 - 1.4$, except on one occasion on Jan 20, 2004 when the airmass was nearly 2.

The spectra were bias subtracted, flatfield corrected, optimally extracted and wavelength calibrated using the IRAF¹ reduction package. The rms scatter in the wavelength calibration was $\approx 0.03 \text{ \AA}$. We further applied a small correction to the wavelength solution by aligning sky lines observed in each of the spectra. Due to variations in seeing, resulting in variable slit losses, the signal-to-noise ratio varied between the spectra from $\approx 80 - 240$ over the wavelength range $5920 - 6520 \text{ \AA}$. Next, we exported the extracted spectra to the data analysis package MOLLY.

In MOLLY the observation times were first corrected to the Heliocentric Julian Date time frame (using UTC times). Next, we normalised and rebinned the spectra to a uniform velocity scale removing the Earth's velocity. Below, we first discuss results obtained using the 1200R+93 grating spectra. We cross-correlated the 1200R+93 grating spectra with spectra of template stars rebinned to the same velocity scale. Nine template star spectra with spectral types ranging from G5-K7 had been obtained with the Keck telescope at similar resolution. We fitted a sinusoid to the measured velocities as a function of time. The fit-parameters are: the phase, the semi-amplitude, and the period of the sinusoid and the systemic velocity. However, since the errors on the velocity represent the statistical error bars only, they do not include the systematic effects which we found to be important (we will come back to this in the Discussion). Therefore, the reduced χ^2 of the fit was much larger than 1. In order to estimate realistic errors on the fit parameters, we increased the size of the error bars such that the reduced χ^2 was close to 1. We found a best-fit period of 9.006 ± 0.007 days, consistent with the orbital period of ≈ 9 days found before (here and below we give 1σ error bars). From this we derive an orbital ephemeris of $\text{HJD} = 2453000.49(8) + N \times 9^d.006(7)$ (UTC) where phase zero is defined as superior conjunction of the neutron star and the number in between brackets denotes the uncertainty in the last digit. The derived ephemeris does not significantly depend on the spectral type of the used template star and is consistent within the errors with the ephemeris given by Mason et al. (1987). We determined a radial velocity semi-amplitude of $99.1 \pm 3.1 \text{ km s}^{-1}$ using the K1V template star HD 124106 (see Figure 1). The radial velocity semi-amplitude does not significantly depend on the spectral type of the template star. I.e. the amplitudes we found varied by 2 km s^{-1} between the minimum and maximum amplitude for template spectral types in the range of G5-K7. We found a systemic velocity of $44.4 \pm 2.4 \text{ km s}^{-1}$.

After correcting each individual spectrum for the ob-

¹ IRAF is distributed by the National Optical Astronomy Observatories

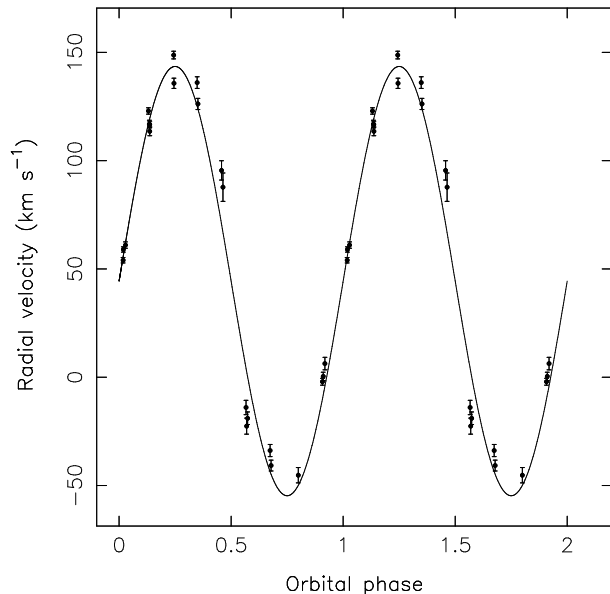


Figure 1. Radial velocity of the companion star in 2S 0921–630. Two cycles have been plotted for clarity. Phase zero is superior conjunction of the neutron star. Overplotted is the best-fit sinusoidal radial velocity curve. The data points are shown with their formal statistical errors only.

served sinusoidal velocity shift appropriate for the orbital phase we created an average spectrum in the frame of the donor star for the data of 2S 0921–630. One can in principle derive the rotational broadening from an optimal subtraction (see for the description of this technique Marsh et al. 1994). However, our data is not well suited for this since the dispersion at which both the template star and the source were observed is relatively low ($\approx 30 \text{ km s}^{-1}$ per pixel in the 5920–6520 Å spectral range for the template star, this spectrum was resampled to the dispersion of $\approx 34 \text{ km s}^{-1}$ per pixel in the 5920–6520 Å spectral range at which the source was observed). Since the template stars were not obtained with the same telescope and instrumental set-up, the instrumental profile will be different from that of the object spectra; together with the low resolution this means that it is not possible to reliably measure the rotational broadening when it is of the order of the spectral resolution. Earlier results on the rotational broadening of $64 \pm 9 \text{ km s}^{-1}$ measured by Shahbaz et al. (1999) showed that this is likely the case. Shahbaz et al. (1999) found a best-fit spectral type of K0 for the companion star; we found that the residuals were smallest when we used the K1 template star HD 124106 (irrespective of broadening). We further found that on average 20 per cent of the light comes from the companion star in the 5920–6520 Å range. In Figure 2 (*Left panel*) we plot the average spectrum in this range, the broadened template star veiled by a source of constant light contributing 80 per cent of the light, and the residuals after subtraction the veiled template star spectrum. We used the spectral range from 5920–6520 Å for the optimal subtraction, however, the range in wavelengths between 6250–6350 Å was masked since it contains a strong interstellar absorption feature.

We further examined whether the contribution of the K1 companion star to the total amount of light in the 5920–6520 Å range varies as a function of the binary orbital phase.

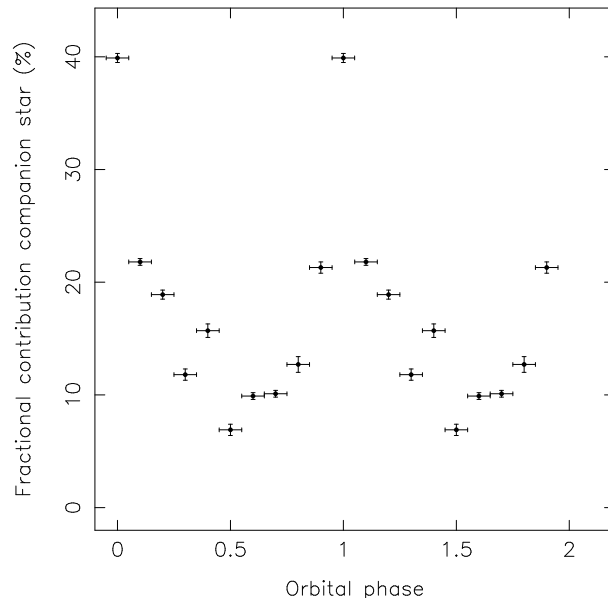


Figure 3. The fractional contribution of the K1 companion star to the total light in the 5920–6520 Å wavelength range as a function of orbital phase. Two cycles have been plotted for clarity. Phase zero is superior conjunction of the neutron star.

We averaged spectra obtained at the same phase using phase bins of width 0.1. We optimally subtracted the template spectrum of the K1 star from the average spectra in each phase bin. The measured fractional contribution of the companion star to the total amount of light in the 5920–6520 Å range is plotted in Figure 3. The large difference in fractional contribution from the K-star between phase 0 and phase 0.1 is difficult to explain.

Besides the stellar absorption lines apparent in the wavelength range 5920–6520 Å shown in the top spectrum of the *Bottom left panel* in Figure 2, additional stellar absorption lines were present in the range 6520–6800 Å (see the *Top left panel* in Figure 2). Furthermore, several emission lines are present in the spectrum. Unfortunately, our observations lack the resolution to resolve these accretion disc lines and hence only one broad emission peak was observed whereas e.g. Shahbaz et al. (1999) observed that the H α and He I emission lines at 6562.76 Å and 6678.15 Å, respectively have the double peaked profile typically observed in accretion disc spectra. We detected a broad emission peak at $\approx 6820 \text{ Å}$ which we could not positively identify. We checked whether CCD defects were present at the position relevant for this wavelength in the flatfield images or in the individual images but none were found.

So far, we have only discussed spectra obtained with the 1200R+93 grating. In Figure 2 (*Bottom right panel*) we show the phase folded average spectra of the 1028z+29 grating in the range between 8300–8900 Å. Clear donor star features such as the Ca II triplet at 8498 Å, 8542 Å, and 8662 Å, and the Mg I line at 8806.75 Å can be seen at orbital phases where the back, non-irradiated side, of the companion star is observed. Furthermore, superimposed on the Paschen disc emission lines, Paschen absorption lines can be seen. Unfortunately, the combined effect of two unresolved broad accretion disc emission lines, a Paschen absorption line and,

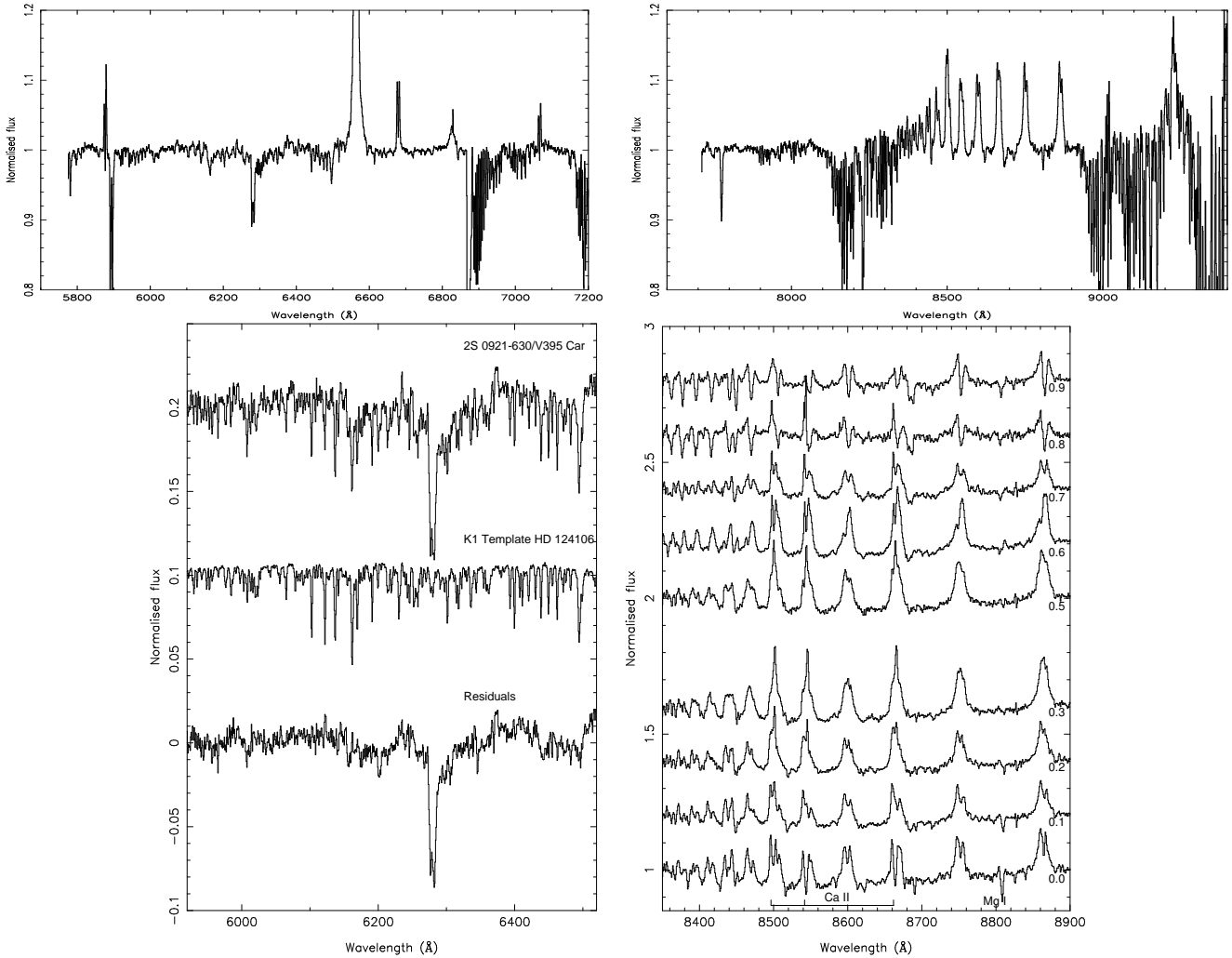


Figure 2. *Top left panel:* The spectrum after averaging all the spectra obtained with the 1200R+93 grating. *Top right panel:* Same as the *top left panel* but using spectra obtained with the 1028z+29 grating. *Bottom left panel:* From top to bottom: The average spectrum of 2S 0921–630 in the range 5920–6520 Å in the frame of the companion star. The K1 template star (HD 124106) spectrum veiled by an accretion disc contribution of 80 per cent. The residual spectrum after subtraction of the veiled template star spectrum. For clarity, the spectra have been normalised and shifted vertically. *Bottom right panel:* Average spectra as a function of phase, the number on the right indicates the centre of the orbital phase bin (there are no spectra in the phase bin from 0.35–0.45 obtained with the 1028z+29 grating hence only 9 spectra are plotted). The CaII and MgI lines from the companion star have been identified below the average spectrum at phase 0.0.

at some wavelengths, and at certain orbital phases, a Ca II absorption line is too difficult to disentangle with the limited resolution data in hand. Therefore, we did not use these spectra for our radial velocity study. Besides the features visible in the *bottom right panel* of Figure 2 we identified two other lines in the 1028z+29 grating spectra; a weak Fe I absorption line complex near 7750 Å and a Paschen emission line at 9229 Å (see the *top right panel* in Figure 2).

3 DISCUSSION

We determined the radial velocity curve of the companion star in 2S 0921–630/V395 Car using VLT/FORS2 spectroscopic observations. A sinusoidal fit to the radial velocity measurements with a semi-amplitude, K_2 , of 99.1 ± 3.1 km s^{-1} and with a systemic velocity, $\gamma = 44.4 \pm 2.4$ km s^{-1} rep-

resents the data well. In these error estimates we artificially increased the error bars on the individual velocity measurements by a factor 4 in order to obtain a reduced χ^2 of the fit close to 1. Before we discuss the implications of the K-velocity, we investigate possible reasons for the large reduced χ^2 obtained when using the formal statistical errors only.

Near quadrature at phase 0.25 the velocity measurements obtained on different nights differ well beyond the statistical errors. From Figure 3 we can see that the companion star contribution to the total amount of light in the 5920–6520 Å range varies as a function of orbital phase. The phasing of this variation suggests that the centre of light emitted by the K-star is likely to be shifted with respect to its centre of mass. An explanation is that the inner side of the companion star is heated by the (X-ray) irradiation coming from (near) the compact object, reducing the equivalent width of the K-star stellar lines in the range 5920–6520

Å (see also e.g. Wade & Horne 1988). This manifests itself in several ways:

(i) a lower fractional contribution to the total amount of light from the K star at e.g. phase 0.5 when using the optimal subtraction technique (e.g. Figure 3)

(ii) an increase in velocity (especially near quadrature) with respect to the velocity associated with the centre of mass of the companion star, since the line profiles will, as a result of the stellar rotation, be preferentially shifted to either a larger red- (phase 0.25) or blue-shift (phase 0.75). Hence, variations in the amount of (X-ray) irradiation between the observations could explain the variations in velocities near quadrature as observed in Figure 1. Since the observations were obtained with at least one day in between, with a baseline of several months, it seems likely that the irradiation changed between the observations.

Furthermore, the velocity measurements around phase 0.5 do not fall on the best-fit sinusoid. Those at phases 0.4–0.5 lay above the best-fit sinusoid, whereas those at phases 0.5–0.6 fall below the curve. This could well be explained by the Rossiter effect (cf. Hilditch 2001). Such deviations occur if the companion star is partially eclipsed by the accretion disc. Such a partial eclipse of the companion star can also help explain the low fraction of light coming from the companion star at phase 0.5 (see Figure 3). The radial velocity measurements at phases just prior to phase 0.5, the partial eclipse of the companion star, are biased to higher, red shifted velocities since the part of the companion star that is eclipsed at those phases is mainly rotating towards the observer. Hence, the rotational broadening of the line will be biased towards the red. The reverse holds for phases just after the partial eclipse.

For the rotational broadening of the stellar lines we take $v \sin i = 64 \pm 9 \text{ km s}^{-1}$ as found by Shahbaz et al. (1999). For a Roche lobe filling companion star the following relation holds: $\frac{v \sin i}{K_2} = 0.46[(1+q)^2 q]^{\frac{1}{3}}$ (e.g. Wade & Horne 1988; q is defined here as M_2 divided by the mass of the compact object, M_X). Before we can determine q , and hence with K_2 the mass of the compact object, we have to take effects of the non-uniform absorption distribution on the stellar surface caused by irradiation into account. To this end, Wade & Horne (1988) developed a so-called K-correction. Following the procedure laid out in Wade & Horne (1988), $K_{2,\text{corr}} = K_{\text{obs}} - \Delta K$. $K_{2,\text{corr}}$ is the corrected observed (K_{obs}) radial velocity semi-amplitude and $\Delta K = f R_2 K_2 / a_2 = f v \sin i$. Here a_2 is the distance between the centre-of-mass of the binary and the centre-of-mass of the companion star and f is a geometrical correction factor less than 1. In the extreme case that the hemisphere facing the compact object does not contribute to the observed stellar absorption lines at all and the other hemisphere has a uniform absorption line strength, $f = \frac{4}{3\pi}$ (Wade & Horne 1988). Since we still have a contribution of the K1 star of around 7 per cent at phase 0.5 we know that this is an overestimation of the K-correction in the case of 2S 0921–630. Hence, applying this upper limit on the K-correction, $\Delta K \leq 26.9 \pm 3.8 \text{ km s}^{-1}$, we get a firm lower limit of $K_{2,\text{corr}} \geq 72.2 \pm 4.9 \text{ km s}^{-1}$. Plugging-in the numbers given above yields $q = 1.32 \pm 0.37$; note that in deriving this we used the equation for R_2/a of Paczynski (1971) which is valid for $0 < q < 0.8$. However, the difference with the equation of Eggleton (1983) is small for $q < 1.7$ and does not

change the result significantly given the large uncertainty in $v \sin i$. The uncertainty in q is dominated by the large error on the rotational velocity. Thus, we find for the minimum mass of the compact object, $M_X \sin^3 i > 1.90 \pm 0.25 M_\odot$. As mentioned in the Introduction, the inclination of 2S 0921–630 must be high. Furthermore, we have presented evidence for a partial eclipse of the companion star. For inclinations, $60^\circ < i < 90^\circ$ (cf. Branduardi-Raymont et al. 1983; Mason et al. 1987) the mass of the compact object is $1.90 \pm 0.25 < M_X < 2.9 \pm 0.4 M_\odot$.

Using $v \sin i = 2\pi R_2 \sin i / P$, we get for the radius of the companion star, R_2 , $R_2 \sin i = 11.4 \pm 1.6 R_\odot$. Under the assumption that the companion star fills its Roche lobe, the mass of the donor star, M_2 , depends only on its radius and the orbital period (cf. Paczynski 1971), which gives $M_2 \sin^3 i = \frac{(R_2 \sin i)^3}{0.234^3 \times P_{\text{orb}}^2}$ (here the orbital period is measured in hours, and the mass and radius of the companion star are in solar units). This gives $M_2 \sin^3 i = 2.5 \pm 1.1 M_\odot$. This M_2 suggests an interesting evolutionary stage of the binary. M_2 is more massive than standard donor stars in LMXBs. Recently, there have been a number of evolutionary calculations (e.g. Tauris et al. 2000; Podsiadlowski et al. 2002) showing that systems with donor masses as high as $\sim 5 M_\odot$ can enter a relatively long phase of mass transfer to a neutron star after the donor has lost most of its mass. 2S 0921–630 would nicely fit in this scenario, evolving along the track of an initial 3–4 M_\odot donor. However, in this evolutionary scenario the current time-averaged mass-transfer rate is expected to be high, certainly super-Eddington. This is at odds with the finding from studying X-ray lines as measured with *Chandra* and *XMM-Newton* that the observed X-ray luminosity of $\sim 10^{36} \text{ erg s}^{-1}$ (for a distance of $\sim 7 \text{ kpc}$) is likely close to the intrinsic source luminosity (Kallman et al. 2003). Perhaps the current mass-transfer rate is much lower than the time-averaged transfer rate, or the donor mass and/or the mass-ratio are overestimated.

Above, we assumed that the companion star is in co-rotation with the binary orbit. Synchronization of the rotational period and the binary period occurs on timescales shorter than the circularization timescale (e.g. Tassoul 1988) and no signs for orbital eccentricity have been found (see Figure 1). Furthermore, using the companion star parameters derived above and equation 7 of Tassoul (1988) we find that the synchronization timescale is $\lesssim 100 \text{ yr}$ for 2S 0921–630, justifying this assumption. We conclude that the compact object in 2S 0921–630 is likely to be a massive neutron star or a low-mass black hole. If indeed the compact object in 2S 0921–630 is a massive neutron star the mass measurement would rule out soft equations of state. Future high resolution optical observations should provide a much more accurate handle on the rotational velocity of the companion star, yielding a more accurate constraint on the mass of the compact object.

ACKNOWLEDGMENTS

Support for this work was provided by NASA through Chandra Postdoctoral Fellowship grant number PF3–40027 awarded by the Chandra X-ray Center, which is operated by the Smithsonian Astrophysical Observatory for NASA under

contract NAS8-39073. DS acknowledges a Smithsonian Astrophysical Observatory Clay Fellowship. GN is supported by PPARC. The use of the spectral analysis software package MOLLY written by Tom Marsh is acknowledged.

van Paradijs, J., McClintock, J. E., 1995, p. 58 in *X-ray Binaries*, eds. W.H.G. Lewin, J. van Paradijs, and E.P.J. van den Heuvel, Cambridge: Cambridge Univ. Press
Wade, R. A., Horne, K., 1988, *ApJ*, 324, 411

REFERENCES

- Bhattacharya, D., 1995, p. 233 in *X-ray binaries*, eds Lewin, van Paradijs, van den Heuvel, Cambridge: Cambridge University Press
- Branduardi-Raymont, G., Corbet, R., Parmar, A. N., Murdin, P. G., Mason, K. O., 1981, *Space Science Reviews*, 30, 279
- Branduardi-Raymont, G., Corbet, R. H. D., Mason, K. O., Parmar, A. N., Murdin, P. G., White, N. E., 1983, *MNRAS*, 205, 403
- Casares, J., Charles, P. A., Kuulkers, E., 1998, *ApJ*, 493, L39
- Casares, J., Dubus, G., Shahbaz, T., Zurita, C., Charles, P. A., 2002, *MNRAS*, 329, 29
- Casares, J., Steeghs, D., Hynes, R. I., Charles, P. A., O'Brien, K., 2003, *ApJ*, 590, 1041
- Chevalier, C., Ilovaisky, S. A., 1981, *A&A*, 94, L3
- Cowley, A. P., Crampton, D., Hutchings, J. B., 1982, *ApJ*, 256, 605
- Eggleton, P. P., 1983, *ApJ*, 268, 368
- Hilditch, R. W., 2001, *An Introduction to Close Binary Stars*, R.W. Hilditch. Cambridge University Press, 2001, 392 pp.
- Jonker, P. G., van der Klis, M., Groot, P. J., 2003, *MNRAS*, 339, 663
- Kallman, T. R., Angelini, L., Boroson, B., Cottam, J., 2003, *ApJ*, 583, 861
- Lattimer, J. M., Prakash, M., 2001, *ApJ*, 550, 426
- Marsh, T. R., Robinson, E. L., Wood, J. H., 1994, *MNRAS*, 266, 137
- Mason, K. O., Branduardi-Raymont, G., Codova, F. A., Corbet, R. H. D., 1987, *MNRAS*, 226, 423
- Nauenberg, M., Chapline, G. J., 1973, *ApJ*, 179, 277
- Nice, D. J., Splaver, E. M., Stairs, I. H., 2003, in *ASP Conf. Ser. 302: Radio Pulsars*, p. 75, astro-ph 0210637
- Nice, D. J., Splaver, E. M., Stairs, I. H., 2004, in *ASP Conf. Ser. TBD: Radio Pulsars*, eds. F.A. Radio & I.H. Stairs, astro-ph 0311296
- Orosz, J. A., Kuulkers, E., 1999, *MNRAS*, 305, 132
- Paczynski, B., 1971, *ARA&A*, 9, 183
- Podsiadlowski, P., Rappaport, S., Pfahl, E. D., 2002, *ApJ*, 565, 1107
- Shahbaz, T., Naylor, T., Charles, P. A., 1993, *MNRAS*, 265, 655
- Shahbaz, T., Kuulkers, E., Charles, P. A., van der Hooft, F., Casares, J., van Paradijs, J., 1999, *A&A*, 344, 101
- Tassoul, J., 1988, *ApJ*, 324, L71
- Tauris, T. M., van den Heuvel, E. P. J., Savonije, G. J., 2000, *ApJ*, 530, L93
- Thorsett, S. E., Chakrabarty, D., 1999, *ApJ*, 512, 288
- Timmes, F. X., Woosley, S. E., Weaver, T. A., 1996, *ApJ*, 457, 834
- van den Heuvel, E. P. J., Bitzaraki, O., 1995, *A&A*, 297, L41